

# Enhanced d(d,p)t fusion reaction in metals

F. Raiola<sup>1,a</sup>, B. Burchard<sup>1</sup>, Zs. Fülöp<sup>2</sup>, Gy. Gyürky<sup>2</sup>, S. Zeng<sup>3</sup>, J. Cruz<sup>4</sup>, A. Di Leva<sup>1</sup>, B. Limata<sup>7</sup>, M. Fonseca<sup>4</sup>, H. Luis<sup>4</sup>, M. Aliotta<sup>5</sup>, H.W. Becker<sup>1</sup>, C. Brogini<sup>9</sup>, A. D'Onofrio<sup>6</sup>, L. Gialanella<sup>7</sup>, G. Imbriani<sup>7</sup>, A.P. Jesus<sup>4</sup>, M. Junker<sup>8</sup>, J.P. Ribeiro<sup>4</sup>, V. Roca<sup>7</sup>, C. Rolfs<sup>1</sup>, M. Romano<sup>7</sup>, E. Somorjai<sup>2</sup>, F. Strieder<sup>1</sup>, and F. Terrasi<sup>6</sup>

<sup>1</sup> Institut für Physik mit Ionenstrahlen, Ruhr-Universität Bochum, Germany

<sup>2</sup> Atomki, Debrecen, Hungary

<sup>3</sup> China Institute of Atomic Energy, Beijing, PRC

<sup>4</sup> Centro de Física Nuclear, Universidade de Lisboa, Portugal

<sup>5</sup> School of Physics, University of Edinburgh, UK

<sup>6</sup> Dipartimento di Scienze Ambientali, Seconda Università di Napoli, Caserta, Italy

<sup>7</sup> Dipartimento di Scienze Fisiche, Università Federico II and INFN, Napoli, Italy

<sup>8</sup> Laboratori Nazionali del Gran Sasso dell'INFN, Assergi, Italy

<sup>9</sup> INFN, Sezione di Padova, Padova, Italy

Received: 21 June 2005 /

Published online: 24 February 2006 – © Società Italiana di Fisica / Springer-Verlag 2006

**Abstract.** The electron screening in the d(d,p)t reaction has been studied for the deuterated metal Pt at a target temperature  $T = 20\text{ °C}$  to  $340\text{ °C}$ , and for Co at  $T = 20\text{ °C}$  and  $200\text{ °C}$ . The enhanced electron screening decreases with increasing temperature, where the data agree with the plasma model of Debye applied to the quasi-free metallic electrons. The data represent the first observation of a temperature dependence of a nuclear cross-section. We also measured the screening effect for the deuterated metal Ti (an element of group 4 of the periodic table) at  $T = -10\text{ °C}$  to  $200\text{ °C}$ : above  $50\text{ °C}$  the hydrogen solubility dropped to values far below unity and a large screening effect became observable. Similarly, all metals of groups 3 and 4 and the lanthanides showed a solubility of a few percent at  $T = 200\text{ °C}$  (compared to  $T = 20\text{ °C}$ ) and a large screening became also observable. Within the Debye model the deduced number of valence electrons per metallic atom agrees with the corresponding number from the Hall coefficient, for all metals investigated.

**PACS.** 25.10.+s Nuclear reactions involving few-nucleon systems – 95.30.-k Fundamental aspects of astrophysics – 25.45.-z  $^2\text{H}$ -induced reactions

## 1 Introduction

The cross-section of a charged-particle-induced nuclear reaction is enhanced at sub-Coulomb energies by the electron clouds surrounding the interacting nuclides, with an enhancement factor [1]

$$f_{lab}(E) = \frac{E}{E + U_e} \exp(-2\pi\eta(E + U_e) + 2\pi\eta(E)), \quad (1)$$

for  $S(E + U_e) \approx S(E)$ , and where  $E$  is the center-of-mass energy,  $\eta(E)$  the Sommerfeld parameter, and  $U_e$  the screening potential energy. The electron screening in d(d,p)t was studied previously for deuterated metals, insulators, and semiconductors, *i.e.* 58 samples in total [2, 3] (see also [4, 5]). As compared to measurements performed with a gaseous  $\text{D}_2$  target ( $U_e = 25\text{ eV}$  [6]), a large screening was observed in the metals (of order  $U_e = 300\text{ eV}$ ),

while a small (gaseous) screening was found for the insulators and semiconductors. An exception was found for the metals of groups 3 and 4 of the periodic table and the lanthanides, which showed a small screening; this is related to their high hydrogen solubility  $y (= 1/x [2, 3])$ , of the order of unity (see also [7]), that gives the deuterated targets of these metals the properties of insulators. Indeed, for the metals with high  $U_e$  values, the solubilities were small (a few percent) leaving the metallic character of the samples essentially unchanged. An explanation of the large screening was suggested [3] by the plasma screening of Debye applied to the quasi-free metallic electrons. The electron Debye radius around the deuterons in the lattice is given by

$$R_D = \sqrt{\frac{\varepsilon_0 k T}{e^2 n_{eff} \rho_a}} = 69 \sqrt{\frac{T}{n_{eff} \rho_a}} \quad [\text{m}], \quad (2)$$

with the temperature  $T$  of the free electrons in units of K,  $n_{eff}$  the number of valence electrons per metallic

<sup>a</sup> e-mail: raiola@ep3.rub.de; for the LUNA Collaboration.

atom, and the atomic density  $\rho_a$  in units of atoms/m<sup>3</sup>. With the Coulomb energy of the Debye electron cloud and a deuteron projectile at  $R_D$  set equal to  $U_e = U_D$ , one obtains

$$U_{e,D} = \frac{e^2}{(4\pi\epsilon_0)R_D} = 2.09 \cdot 10^{-11} \sqrt{\frac{n_{eff}\rho_a}{T}} \quad [\text{eV}]. \quad (3)$$

A comparison of the calculated and observed  $U_e$  values led to  $n_{eff}$ , which was for most metals of the order of unity. The acceleration mechanism of the incident positive ions leading to the high observed  $U_e$  values is thus the Debye electron cloud at the small radius  $R_D$ , about one tenth of the Bohr radius. The  $n_{eff}$  values were compared with those deduced from the known Hall coefficient [8]: within 2 standard deviations the two quantities agreed for all metals. A critical test of the Debye model is the predicted temperature dependence  $U_e(T) \propto T^{-1/2}$  (see also below); for deuterated Pt at  $T = 20^\circ\text{C}$  and  $100^\circ\text{C}$  the data agreed with prediction [3].

It is known [7] that the hydrogen solubility in metals decreases with increasing temperature. Thus, at higher temperatures the solubility of the metals of groups 3 and 4 and the lanthanides may be low enough (a few percent) that large  $U_e$  values can be observed and thus new  $n_{eff}$  values deduced. With the assumption that the temperature-dependent solubility  $y(T)$  affects directly  $n_{eff}$ , one obtains

$$U_{e,D}(T) = \begin{cases} \frac{1}{4.78 \cdot 10^{10}} \sqrt{\frac{(n_{eff}(T)(1-y(T))\rho_a}{T}} & y(T) \leq 1, \\ 0, & y(T) > 1, \end{cases} \quad [\text{eV}], \quad (4)$$

where a temperature dependence of  $n_{eff}(T)$  is also taken into account. We report on the measurement of such temperature effects.

## 2 Setup and experimental procedure

The equipment, procedures, and data analysis have been described elsewhere [2,3]. Briefly, the surface of a given sample was—in a first step—cleaned *in situ* by Kr sputtering at 35 keV removing typically about 300 monolayers. The sample was—in a second step—deuterated at a given deuteron energy until a saturated yield was reached. This implantation procedure was repeated over the full energy range of the planned experiment taking typically about 4 days of running. Finally, the observed thick-target yield curve was differentiated to arrive at a thin-target yield curve, which was fitted using 2 free parameters,  $y(T)$  and  $U_e(T)$ : the absolute yield provided information on the hydrogen solubility  $y(T)$  and the energy dependence of the data gave the screening potential energy  $U_e(T)$ . We tested also the stability of the solubility against diffusion by switching the deuteron beam off for an extended period (typically 6 hours); the subsequent yield measurement was unchanged within experimental uncertainty indicating a stable solubility, both at room temperature and elevated temperatures. For the present measurements at elevated temperatures a new target holder was

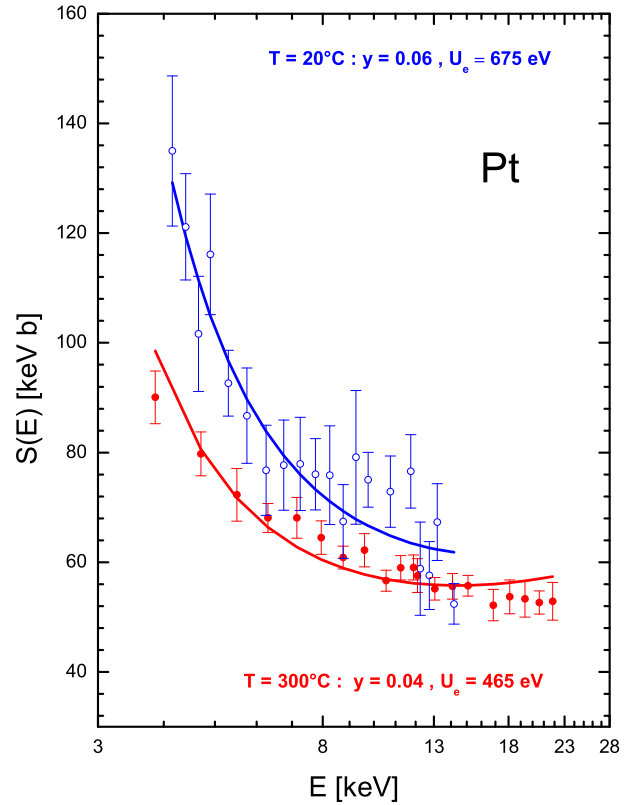


**Fig. 1.**  $S(E)$  factor of d(d,p)t for Pt at  $T = 20^\circ\text{C}$  and  $300^\circ\text{C}$ , with the deduced solubilities  $y$ . The curves through the data points include the bare  $S(E)$  factor and the electron screening with the  $U_e$  values given.

designed [9]. It consists of a diamond plate coated with a metallic layer (area  $A = 20 \times 20 \text{ mm}^2$ , thickness  $t = 1 \text{ mm}$ ) and heated by current flow. A given metal sheet ( $A = 15 \times 17 \text{ mm}^2$ ) is placed on top of the diamond plate with interim plates (from bottom to top) of MACOR ( $t = 1 \text{ mm}$ ), Cu ( $t = 3 \text{ mm}$ ), and MACOR ( $t = 1 \text{ mm}$ ). At the center of the top MACOR plate there is a hole of  $\varnothing = 5 \text{ mm}$  diameter, filled with another diamond of cylindrical shape and 2 mm height: it provides the thermal contact to the metal foil. The metal foil is electrically insulated for current measurement. Thermal elements measure the temperature at the diamond plate and the metal foil (near the area of the ion beam spot). The Si detectors in close geometry to the metal foil were cooled to  $0^\circ\text{C}$  using an Ultra Kryomat. The beam direction and spot on target were defined by 2 apertures, one of  $\varnothing = 3 \text{ mm}$  at a distance  $d = 62 \text{ cm}$  from the target and the other of  $\varnothing = 6 \text{ mm}$  at  $d = 280 \text{ cm}$ ; an electric quadrupole triplet placed between the 2 apertures was used to focus the beam. The beam current on target was kept below  $2 \mu\text{A}$  leading to a negligible influence on the target temperature (less than  $2^\circ\text{C}$  variation).

## 3 Temperature dependence of Pt and Co

We measured the screening effect for the metal Pt at a target temperature between  $T = 20^\circ\text{C}$  and  $340^\circ\text{C}$ , and

**Table 1.** Summary of the results.

Material <sup>a</sup>	$T(^{\circ}\text{C})$	$U_e(\text{eV})^b$	Solubility $y^c$	$n_{eff}^b$	$n_{eff}(\text{Hall})^d$
<b>Groups 3 and 4 and lanthanides</b>					
Ce	200	200±50	0.11	1.5±0.7	(1.2±0.2)
Dy	200	340±70	0.09	4.9±2.0	1.5±0.3
Er	200	360±80	0.05	4.3±1.9	6±1
Eu	200	120±60	0.05	0.8±0.8	
Gd	200	340±85	0.08	4.2±2.1	2.2±0.4
Hf	200	370±70	0.04	4.0±1.5	(3.2±0.6)
Ho	200	165±50	0.07	0.9±0.5	
La	200	245±70	0.09	2.4±1.4	2.9±0.6
Lu	200	265±70	0.08	2.2±1.2	3.4±0.7
Nd	200	190±50	0.08	1.4±0.7	(2.2±0.4)
Sc	200	320±50	0.11	2.6±0.8	2.2±0.4
Sm	200	314±60	0.08	3.5±1.3	10±2
Tb	200	340±80	0.18	3.9±1.8	
Tm	200	260±80	0.05	2.2±1.4	1.0±0.2
Y	200	270±75	0.09	2.6±1.4	2.7±0.5
Yb	200	110±40	0.13	0.4±0.3	(0.6±0.1)
Zr	200	205±70	0.13	1.1±0.7	(1.1±0.2)
<b>Insulators</b>					
C	200	≤ 50	0.15		
<b>T-dependence of Co and Pt</b>					
Co	20	640±70	0.14		
	200	480±60	0.02		
Pt	20	675±50	0.06		
	100	530±40	0.06		
	200	530±40	0.05		
	300	465±38	0.04		
	340	480±70	0.04		
<b>T-dependence of Ti</b>					
Ti	-10	≤ 30	2.1		
	50	≤ 50	1.1		
	100	250±40	0.26		
	150	295±40	0.23		
	200	290±65	0.20	1.7±0.7	4±1

<sup>a</sup> For details see ref. [9].

<sup>b</sup> Error contains no systematic uncertainty in energy dependence of stopping power.

<sup>c</sup> Estimated uncertainty is about 20%.

<sup>d</sup> From the observed Hall coefficient, with an assumed 20% error; the numbers in brackets are for hole carriers.

for Co at  $T = 20^{\circ}\text{C}$  and  $200^{\circ}\text{C}$ . Both metals have a solubility of a few percent at all  $T$  of the present work. The astrophysical  $S(E)$  factor obtained at  $T = 20^{\circ}\text{C}$  and  $300^{\circ}\text{C}$  for Pt is shown in fig. 1. The results for Co and Pt are given in table 1 and the  $U_e(T)$  values for Pt are plotted in fig. 2 together with the expected dependence  $U_e(T) \propto T^{-1/2}$  (dotted curve). All data show a decrease of the screening, *i.e.* the  $U_e$  value, with increasing temperature. Over the present temperature range, the reported Hall coefficient for Pt increases by about 20% [8,10] leading to a corresponding decrease in  $n_{eff}$ , which we took into account (solid curve in fig. 2); there is good agreement between observation and expectation. The data represent the first observation of a temperature dependence of a nuclear cross-section.

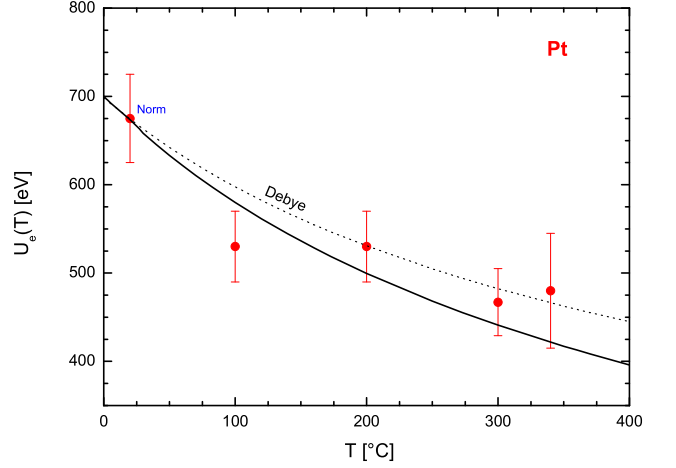


**Fig. 2.** The observed values  $U_e(T)$  for Pt is shown as a function of sample temperature  $T$ . The dotted curve represents the prediction of the Debye model (eq. (5)) and the solid curve includes the observed  $T$ -dependence of the Hall coefficient [8, 10], *i.e.*  $n_{eff}(T)$ .

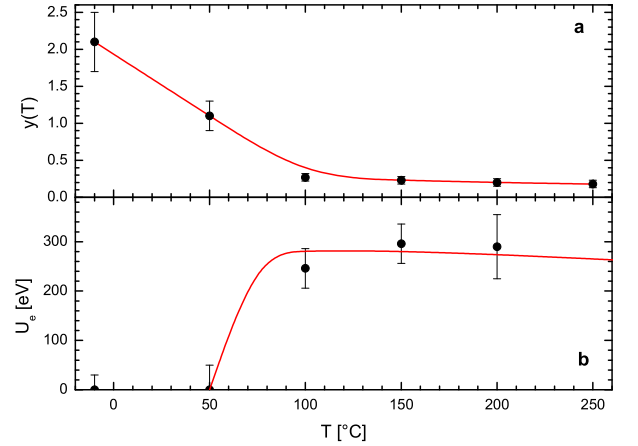


**Fig. 3.** a) Hydrogen solubility  $y(T)$  in Ti as a function of sample temperature  $T$ . The curve through the data points is to guide the eye only. b) Observed  $U_e(T)$  values as a function of  $T$ . The curve through the data points uses eq. (4) together with the observed  $y(T)$  values and  $n_{eff}(\text{Ti}) = 1.7$ .

#### 4 Temperature dependence of metals with high solubility at $T = 20^{\circ}\text{C}$

We studied the electron screening effect for the deuterated metal Ti (group 4) at  $T = -10^{\circ}\text{C}$  to  $200^{\circ}\text{C}$ , in steps of  $50^{\circ}\text{C}$ . The deduced solubility  $y(T)$  is shown in fig. 3 and shows a sizable decrease with increasing temperature, where above  $50^{\circ}\text{C}$  the solubility reaches values below unity and thus an enhanced screening should be observable at these higher temperatures. The observed  $U_e$  values (fig. 3b) verify this expectation, where the solid curve in fig. 3b uses eq. (4) including the observed  $y(T)$ -dependence and  $n_{eff}(\text{Ti}) = 1.7$  (table 1); the analysis indicates a maximum effect around  $100^{\circ}\text{C}$ . Note that a

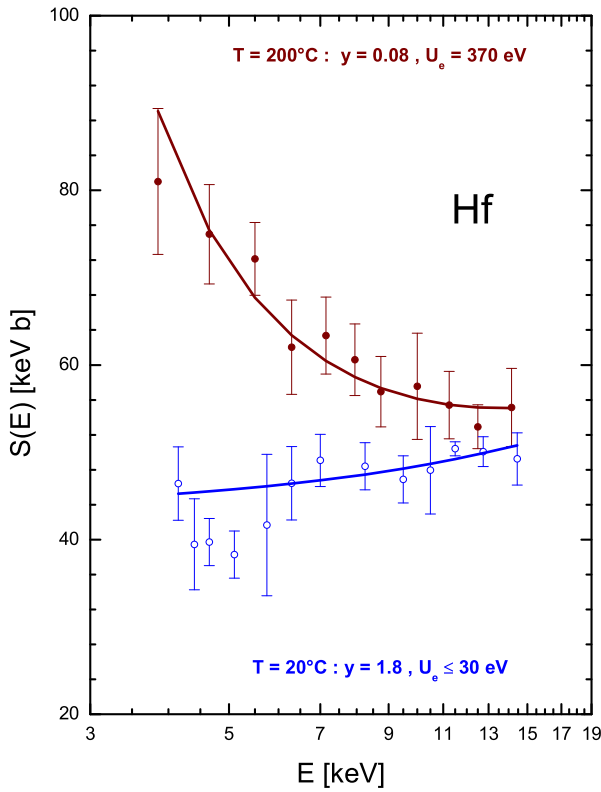


**Fig. 4.**  $S(E)$  factor of d(d,p)t for Hf at  $T = 200^\circ\text{C}$  and  $T = 20^\circ\text{C}$ , with the deduced solubilities  $y$ . The curve for  $T = 20^\circ\text{C}$  represents well the bare  $S(E)$  factor, while the curve for  $T = 200^\circ\text{C}$  includes the electron screening with the  $U_e$  value given.

solubility of 10% leads to a 5% reduction in the maximum value of  $U_e$ , according to eq. (4).

Finally, all metals of groups 3 and 4 and the lanthanides have been studied at  $T = 200^\circ\text{C}$ . The astrophysical  $S(E)$  factor obtained at  $T = 200^\circ\text{C}$  for Hf is compared in fig. 4 with that obtained at  $T = 20^\circ\text{C}$ : at  $T = 200^\circ\text{C}$  the solubility is reduced to a few percent and a large screening became observable, similarly as for Ti. In fact, all these metals exhibited a large reduction in solubility and thus showed a large screening, as expected according to eq. (4). The results for all metals are summarized in table 1, which also compares the deduced  $n_{eff}$  values with those from the Hall coefficient: there is again an agreement between both quantities within two standard deviations, for all metals of the present and previous work [3], *i.e.* 49 metals in total. As a consistency test we also studied the insulator C at  $T = 200^\circ\text{C}$ : the solubility

decreased from 0.35 ( $T = 20^\circ\text{C}$ ) to 0.15, but no enhanced screening was observed, as expected for an insulator with  $n_{eff} = 0$  (eq. (4)).

## 5 Discussion

All data on the enhanced electron screening in deuterated metals can be explained quantitatively by the Debye model applied to the quasi-free metallic electrons. It was argued [3] that most of the conduction electrons are frozen by quantum effects and only electrons close to the Fermi energy ( $E_F$ ) actually should contribute to screening, with

$$n_{eff}(T) = 0.67 \frac{kT}{E_F} \propto T, \quad (5)$$

and thus there should be essentially no temperature dependence for  $U_{e,D}$ . However, this argument applies only to insulators and semiconductors with a finite energy gap, while for metals there is no energy gap and the Fermi energy lies within the conduction band. Note that the observed  $n_{eff}(T)$  from the Hall coefficient decreases with increasing  $T$ , *e.g.* for Pt, contrary to eq. (5). Clearly, an improved theory is highly desirable to explain why the simple Debye model appears to work so well. Without such a theory, one may consider the Debye model as a powerful parameterization of the data.

This work was supported by BMBF (05CL1PC1), DFG (Ro429/31, 436Ung113), AvH (V-8100/B-ITA1066680), OTKA (T42733, T49245), China (2003CB716704), Portugal (FNU-45092-2002) and Dynamitron-Tandem-Laboratorium.

## References

1. H.J. Assembaum, K. Langanke, C. Rolfs, Z. Phys. **327**, 461 (1987).
2. F. Raiola, *et al.*, Eur. Phys. J. A **13**, 377 (2002).
3. F. Raiola, *et al.*, Eur. Phys. J. A **19**, 283 (2004).
4. J. Kasagi *et al.*, J. Phys. Soc. Jpn. **71** 2881 (2002); J. Kasagi *et al.*, J. Phys. Soc. Jpn. **73**, 608 (2004).
5. K. Czerski, A. Huke, A. Biller, P. Heide, M. Hoefl, G. Ruprecht, Europhys. Lett. **54**, 449 (2001).
6. U. Greife, F. Gorris, M. Junker, C. Rolfs, D. Zahnov, Z. Phys. A **351**, 107 (1995).
7. A. Züttel, Naturwissenschaften **91**, 157 (2004).
8. C.M. Hurd, *The Hall Effect in Metals and Alloys* (Plenum Press, 1972).
9. F. Raiola, PhD Thesis, Ruhr-Universität Bochum (2005).
10. Landolt-Börnstein, Vol. **II.6** (Springer, Berlin, 1959).